Influence of a Ta spacer on the magnetic and transport properties of perpendicular magnetic tunnel junctions

Léa Cuchet, Bernard Rodmacq, Stéphane Auffret, Ricardo C. Sousa, Clarisse Ducruet, Bernard Dieny

Influence of a Ta spacer on the magnetic and transport properties of perpendicular magnetic tunnel junctions

Léa Cuchet, Bernard Rodmacq, Stéphane Auffret, Ricardo C. Sousa, Clarisse Ducruet, and Bernard Dieny
SPINTEC, UMR8191, CEA/CNRS/UJF/G-INP, INAC-CEA Grenoble, 38054 Grenoble Cedex, France

(Received 25 June 2013; accepted 14 July 2013; published online 29 July 2013)

Ultrathin Ta layers were inserted in the bottom hard (Co/Pt)/Ta/CoFeB/MgO magnetic electrode of perpendicular magnetic tunnel junctions. The magnetization of the top part of this electrode abruptly falls in-plane when the Ta thickness exceeds 0.45 nm. This results from the balance between the various energy terms acting on this layer (exchange-like coupling through Ta, demagnetizing energy, and perpendicular anisotropy at the CoFeB/MgO interface). For small Ta thicknesses, this insertion leads to a strong improvement of the tunnel magnetoresistance, as long as the magnetization of all layers remains perpendicular-to-plane. © *2013 AIP Publishing LLC*. [http://dx.doi.org/10.1063/1.4816968]

Spin Transfer Torque Random Access Memories (STT-RAM) represent a promising type of non-volatile memories that are particularly attractive because of their unique combination of qualities: high write speed (a few ns), low write energy (a few pJ), infinite endurance ($>10^{16}$ write cycles), small size ($\sim 6F^2$, F being the feature size associated with the technology node). A lot of work has been carried out on Magnetic Tunnel Junctions (MTJs), since first-principle calculations predicted in 2001[1] that a very large Tunnel MagnetoResistance (TMR) ratio could be reached for junctions based on a crystalline MgO insulating barrier and bcc Fe or FeCo magnetic electrodes. This phenomenon was experimentally evidenced in 2004 for Fe/MgO/Fe epitaxial structures[2] as well as for CoFe/MgO/CoFe sputtered junctions,[3] with a TMR ratio around 180%. Later on, due to an easier implementation, research focused on sputtered MTJs comprising amorphous CoFeB electrodes that have the advantage, after annealing, to yield the right bcc (100) texture.[4] These structures enabled getting a TMR ratio of the order of a few hundreds of percent.

Initially, these junctions were based on magnetic electrodes with in-plane magnetization, for which the stability of the magnetic coding is achieved, through shape anisotropy, by giving to the memory cell an elliptical shape (typical aspect ratio of the order of 2 to 2.5). However, the resulting energy barrier only yields sufficient thermal stability down to cell size of the order of $65 \times 170\,nm^2$. More recently, MTJs with perpendicularly magnetized electrodes (p-MTJs) have attracted a lot of interest. This is due to the expected higher storage densities and thermal stability which can be achieved with this kind of structures. Besides, for a given retention time of the information, it was shown that lower current densities are needed with p-MTJs written by STT switching compared to in-plane magnetized MTJs.[5] To introduce perpendicular magnetic anisotropy (PMA) in such tunnel junctions, one may use Co/Pt or Co/Pd multilayers.[6,7] In addition, it was shown more than ten years ago that the magnetic metal/oxide interface also contributes to PMA,[8,9] and more recently that the interfacial properties of both seed and capping layers can have a significant impact on PMA.[6,10]

Even if Co/Pt (Pd) multilayers are a good choice to induce or reinforce PMA in CoFeB layers by exchange-like coupling, it is necessary to introduce a spacer between both magnetic layers.[6,11] Indeed, it is very difficult to get the right bcc (100) texture for CoFeB electrodes when they directly grow on fcc (111) Pt (Pd) or hcp (0001) Co layers. The role of this spacer is thus to structurally decouple the two magnetic entities (Co/Pt multilayer and CoFeB layer), thus allowing crystallization of the CoFeB layers from the MgO side with the adequate bcc (100) texture. In addition, this spacer has a second beneficial effect, since it attracts, upon annealing, boron atoms out of the CoFeB layer and away from the CoFeB/MgO interface.[12] However, if this spacer gets too thick, it also magnetically decouples the magnetic layers, so that the PMA coming from the (Pt/Co) multilayer can no longer help pulling the CoFeB magnetization out-of-plane. Sokalski *et al.*[13] recently showed on FeCoB/Ta/FeCoB/MgO electrodes that it is possible to find a window of Ta thickness allowing both strong PMA and strong ferromagnetic coupling between the two FeCoB layers. However, in that case PMA is much smaller than that obtained thanks to exchange coupling to Co/Pt (Pd) multilayers.

In this letter, we present the effect of a thin Ta insertion layer in the bottom hard electrode of perpendicular tunnel junctions on their magnetic and transport properties. In that hard electrode, the perpendicular Co/Pt multilayer is exchange-coupled to a CoFeB layer through this thin Ta layer of varying thickness. We show that the Ta insertion initially greatly improves the TMR ratio, up to a critical thickness of 0.45 nm, above which magnetic decoupling through Ta leads to a reorientation of the CoFeB magnetization from out-of-plane to in-plane, with a corresponding abrupt decrease of the TMR ratio.

Samples were deposited by magnetron sputtering under an Ar pressure of 2.10^{-3} millibar. The stack of the junctions is the following (thicknesses are given in nm): $Si/SiO_2/Ta3/Pt5/(Co0.5/Pt0.4)_5/Co0.5/Tax_{Ta}/Co_{60}Fe_{20}B_{20}1.2/MgO/Fe_{72}Co_8B_{20}1.2/Ta1/Pt2$, where the Ta thickness x_{Ta} varies between 0 and 0.9 nm. We use two compositions of amorphous CoFeB alloy that we will later call CoFeB and FeCoB, for Co-rich

and Fe-rich alloys, respectively. The MgO barrier is obtained by natural oxidation of a 0.9 nm thick metallic layer of Mg under an oxygen pressure of 150 mbar, for 10 s. On top of this oxidized layer, a second layer of 0.5 nm of Mg is then deposited. Samples were annealed under 10^{-6}millibar vacuum at 300 °C for 1 h without applied magnetic field. Magnetic characterizations were performed using an Extraordinary Hall Effect (EHE) setup and by Vibrating Sample Magnetometry (VSM), the magnetic field being applied perpendicular to the sample plane. We remind that the extraordinary part of the Hall resistance is proportional to the perpendicular component of the magnetization. Macroscopic transport measurements were performed using the CIPT technique[14] on identical samples deposited in the same run on a 60 nm thick CuN buffer layer and subsequently covered by a 15 nm thick Ru layer, in order to adapt the resistance of bottom and top electrodes to that of the MgO barrier.

A typical magnetic hysteresis loop without Ta insertion ($x_{Ta} = 0$) is shown in Figure 1. Transitions of the top magnetically soft FeCoB and the bottom hard electrodes are visible, both of them exhibiting perpendicular anisotropy. A minor loop is realized on the top electrode and the corresponding curve is shown in red in Figure 1. It can be seen that this loop is not centered on zero field but is slightly shifted towards positive fields (coming from positive saturation), showing that an antiferromagnetic coupling exists through the MgO barrier between the two magnetic electrodes. Such an antiferromagnetic coupling has already been observed in perpendicular magnetic junctions, and arises from Néel-type coupling for structures with strong perpendicular anisotropy.[15,16] For this sample without Ta insertion, the coupling field H_{cpl} amounts to −80 Oe, with the usual sign convention.

The same measurements were performed for increasing values of the Ta insertion thickness x_{Ta} and Figure 2 shows the corresponding loops for $x_{Ta} = 0.4$, 0.5, and 0.6 nm. In order to facilitate the comparison between samples, the three curves are normalized to their maximum Hall resistance value, and only part of the hysteresis cycle (from +4kOe to −1kOe) is shown. One observes the appearance of a hard axis component in the loops for $x_{Ta} = 0.5$ and 0.6 nm. This component is attributed to the CoFeB layer deposited on top

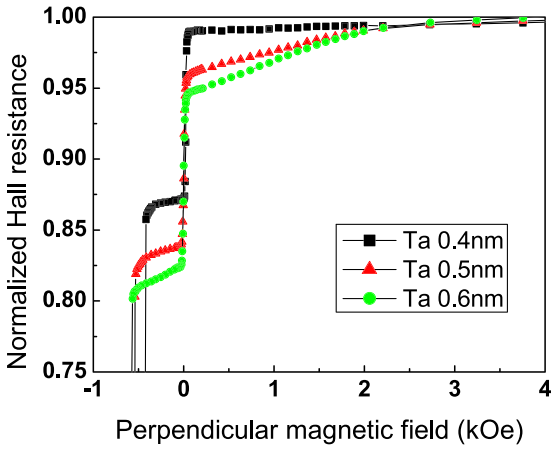

FIG. 2. Part of the EHE hysteresis loops (between +4 and −1kOe) for $x_{Ta} = 0.4$, 0.5, and 0.6 nm.

of the Ta spacer, whose magnetization abruptly decouples from that of the bottom Co/Pt multilayer and falls in-plane. The field required to pull back this layer in the perpendicular direction amounts to about 3 kOe. This reorientation of the anisotropy direction is not observed in the work of Sokalski *et al.*[13] since in their case the CoFeB layer on top of the Ta insertion is thin enough to keep perpendicular anisotropy by itself, even when it is fully decoupled from the CoFeB layer deposited below the Ta layer. However, the critical Ta thickness they quote is similar to the one we observe in our samples.

Figure 3 presents the variation of the amplitude of this in-plane signal (normalized to the Hall amplitude of the bottom electrode) as a function of the Ta insertion thickness. For thicknesses up to 0.45 nm, no in-plane component is visible on the hysteresis loop, whereas for thicknesses above 0.55 nm this component becomes constant with an amplitude of about 4.5% of the Hall signal. For $x_{Ta} = 0.5$ nm, the constant level of amplitude is not yet reached which leads us to assume that the system is in an intermediate state for this thickness: magnetization is not homogeneous in the whole CoFeB layer and some parts (probably because of the

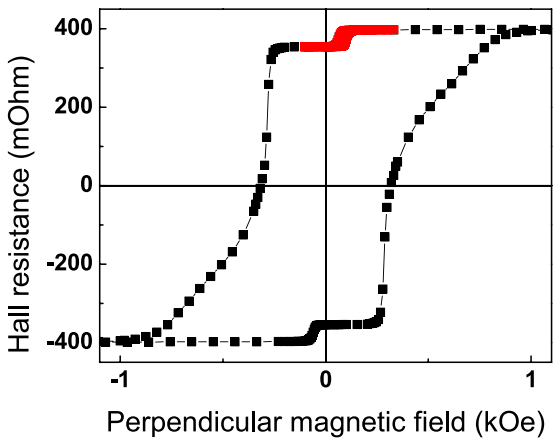

FIG. 1. Typical EHE loop for $x_{Ta} = 0$ nm. The red curve shows the minor cycle of the soft layer.

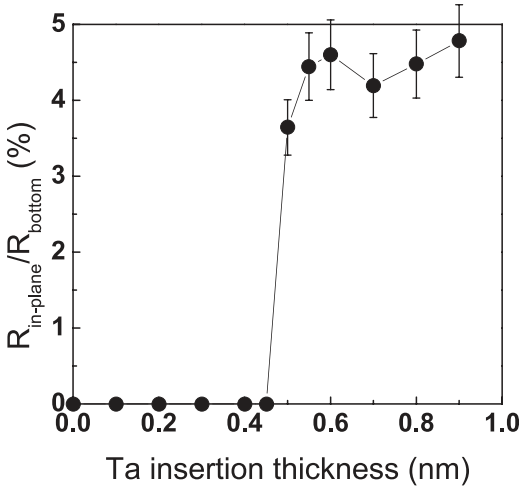

FIG. 3. Relative Hall contribution of the in-plane component of the bottom electrode as a function of the Ta insertion thickness.

roughness of the layers) remain with a perpendicular anisotropy. Let us note that the Hall amplitude of the in-plane component is much smaller than its expected magnetization contribution (about 30% assuming equal Co and CoFeB magnetizations). This comes from the fact that the Hall coefficient of the Ta/CoFeB/MgO layer is much smaller than that of the Pt/Co/Pt ones due to a weaker spin-orbit coupling in the CoFeB layer as compared to the (Co/Pt) multilayer. However, complementary VSM measurements give the expected relative magnetic contribution of both perpendicular and in-plane components of the bottom magnetic electrode on both sides of the Ta insertion layer.

Figure 4(a) shows the variation of the anisotropy field of the in-plane contribution as a function of the Ta insertion thickness (i.e., the field needed to orient perpendicularly the magnetization of the in-plane CoFeB layer). Following the usual convention, this field is given with a negative sign. As we have shown before, this in-plane contribution appears for $x_{Ta} = 0.5$ nm. The anisotropy field then progressively decreases with increasing Ta thickness, from about −3kOe for $x_{Ta} = 0.5$ nm to −1kOe for $x_{Ta} = 0.9$ nm. This can be explained by an increasing perpendicular anisotropy of the in-plane magnetized CoFeB layer deposited on a Ta layer of increasing thickness. Ta presents the ability to attract boron from CoFeB during annealing.[12] As the boron atoms diffuse away from the CoFeB/MgO interface, PMA is further improved.[10,17,18] Thus, when the thickness of the Ta insertion increases, it becomes easier to reorient the in-plane magnetized CoFeB layer towards the perpendicular direction. Although papers report some PMA contribution of the Ta/CoFeB interface,[6,10] others indicate that PMA solely comes from the CoFeB/MgO one, this PMA being enhanced by a better growth on that Ta seed layer.[19] The constant relative Hall amplitude above $x_{Ta} = 0.55$ nm observed in Figure 3, confirmed by VSM measurements, excludes the possibility of a progressive alloying between the Ta and CoFeB layers, which would lead to a decrease of the effective magnetic thickness and thus to a decrease of the anisotropy field.

As already pointed out in Figure 1, there is antiferromagnetic coupling between the magnetic electrodes through the MgO barrier. The evolution of this parameter is representative of the effect of both increasing Ta layer thickness and magnetic anisotropy reorientation of the bottom CoFeB

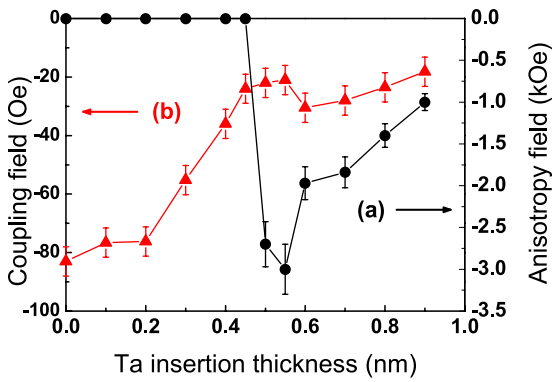

FIG. 4. Variation as a function of the Ta insertion thickness of (a) the perpendicular anisotropy field of the in-plane contribution (black circles, right-hand scale) and (b) the coupling field between the bottom and top magnetic layers through the MgO barrier (red triangles, left-hand scale).

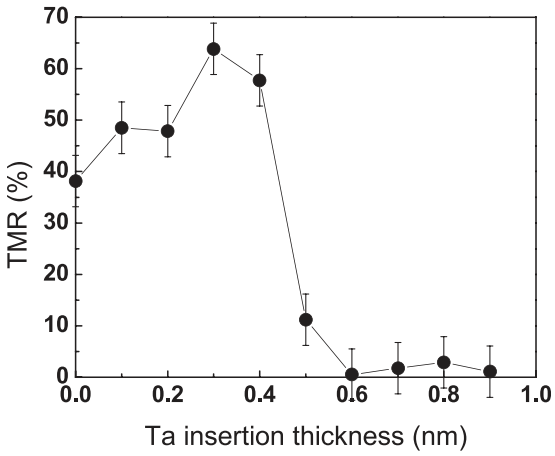

FIG. 5. TMR evolution as a function of the Ta insertion thickness.

layer. Figure 4(b) shows the evolution of the coupling field H_{cpl} as a function of the Ta thickness. Since this coupling field is linked to the coupling energy J_{cpl} through $J = H_{cpl}M_s t$, where M_s and t refer to the magnetization and thickness of the top soft FeCoB magnetic electrode (both parameters being constant in the present case), the variation of the coupling field directly reflects that of the coupling energy. Increasing the Ta insertion thickness leads to a progressive decrease of the antiferromagnetic coupling energy, as a consequence of the decreasing roughness of the MgO barrier thanks to the beneficial effect of the underlying Ta layer. These results agree with those recently reported.[19] Above a Ta thickness of 0.5 nm, when the magnetization of the CoFeB layer is in-plane, the coupling field remains constant at about −20 Oe. This non-zero asymptotic limit probably results from remaining stray fields from both electrodes, their magnetization not being perfectly orthogonal to each other as a consequence of interfacial roughness.

Finally, transport measurements were performed on the samples with a CIPT measurement tool. After magnetic saturation of the samples in a magnetic field of 1.5 kOe, the electrical resistance of the samples was measured with applied magnetic fields of +/−150 Oe, large enough to saturate the magnetization of the top FeCoB soft layer in the positive or negative perpendicular direction. The TMR ratio as a function of the Ta insertion thickness is presented in Figure 5. The TMR variation confirms the magnetic results that have been shown previously. The TMR ratio is around 40% without Ta insertion, and increases with increasing Ta thickness up to 70% for a Ta thickness of 0.4 nm. This reflects the improvement of the texture of the CoFeB layer thanks to the Ta insertion. Above $x_{Ta} = 0.45$ nm, the TMR ratio abruptly decreases, which agrees with the reorientation of the CoFeB magnetization direction from perpendicular to in-plane deduced from the magnetic measurements. As a matter of fact, switching from up to down the magnetization of the soft top magnetic layer does not modify the angle it makes with that of the now in-plane bottom electrode (90°), leading to zero magnetoresistance.

In conclusion, we show in this letter a clear correlation between magnetic and transport properties of perpendicular magnetic tunnel junctions when a thin Ta layer is inserted in the hardest magnetic electrode in order to structurally decouple the growth of the CoFeB layer from that of the

underlying Co/Pt multilayer. The Ta insertion reveals its great efficiency up to 0.45 nm, leading to an increase of the TMR ratio from 40% to 70%. Above that critical Ta thickness, TMR abruptly decreases due to the reorientation of the magnetization of the CoFeB layer from perpendicular-to-plane to in-plane, as a consequence of its magnetic decoupling from the Co/Pt multilayer. A good compromise can be found for a Ta thickness around 0.4 nm. For such a thickness, it is possible to decouple the growth of CoFeB from the underlying multilayer while maintaining perpendicular anisotropy of the whole structure, both conditions leading to high TMR values.

We acknowledge the financial support from the ANR (French National Research Agency) under project ANR-NANO PATHOS and from the European Union under the ERC HYMAGINE project n° 246942.

[1]W. H. Butler, X.-G. Zhang, T. C. Schulthess, and J. M. MacLaren, Phys. Rev. B **63**, 054416 (2001).
[2]S. Yuasa, T. Nagahama, A. Fukushima, Y. Suzuki, and K. Ando, Nature Mater. **3**, 868–871 (2004).
[3]S. S. P. Parkin, C. Kaiser, A. Panchula, P. M. Rice, B. Hughes, M. Samant, and S.-H. Yang, Nature Mater. **3**, 862–867 (2004).
[4]D. D. Djayaprawira, K. Tsunekawa, M. Nagai, H. Maehara, S. Yamagata, N. Watanabe, S. Yuasa, Y. Suzuki, and K. Ando, Appl. Phys. Lett. **86**, 092502 (2005).
[5]O. G. Heinonen and D. V. Dimitrov, J. Appl. Phys. **108**, 014305 (2010).
[6]D. C. Worledge, G. Hu, D. W. Abraham, J. Z. Sun, P. L. Trouilloud, J. Nowak, S. Brown, M. C. Gaidis, E. J. O'Sullivan, and R. P. Robertazzi, Appl. Phys. Lett. **98**, 022501 (2011).
[7]K. Mizunuma, M. Yamanouchi, S. Ikeda, H. Sato, H. Yamamoto, H.-D. Gan, K. Miura, J. Hayakawa, F. Matsukura, and H. Ohno, Appl. Phys. Express **4**, 023002 (2011).
[8]S. Monso, B. Rodmacq, S. Auffret, G. Casali, F. Fettar, B. Gilles, B. Dieny, and P. Boyer, Appl. Phys. Lett. **80**, 4157–4159 (2002).
[9]B. Rodmacq, A. Manchon, C. Ducruet, S. Auffret, and B. Dieny, Phys. Rev. B **79**, 024423 (2009).
[10]H. Yamamoto, J. Hayakawa, K. Miura, K. Ito, H. Matsuoka, S. Ikeda, and H. Ohno, Appl. Phys. Express **5**, 053002 (2012).
[11]A. Natarajarathinam, R. Zhu, P. B. Visscher, and S. Gupta, J. Appl. Phys. **111**, 07C918 (2012).
[12]X. Kozina, S. Ouardi, B. Balke, G. Stryganyuk, G. H. Fecher, C. Felser, S. Ikeda, H. Ohno, and E. Ikenaga, Appl. Phys. Lett. **96**, 072105 (2010).
[13]V. Sokalski, M. T. Moneck, E. Yang, and J.-G. Zhu, Appl. Phys. Lett. **101**, 072411 (2012).
[14]D. C. Worledge and P. L. Trouilloud, Appl. Phys. Lett. **83**, 84–86 (2003).
[15]J. Moritz, F. Garcia, J.-C. Toussaint, B. Dieny, and J.-P. Nozières, Europhys. Lett. **65**, 123–129 (2004).
[16]L. E. Nistor, B. Rodmacq, S. Auffret, A. Schuhl, M. Chshiev, and B. Dieny, Phys. Rev. B **81**, 220407 (2010).
[17]L. E. Nistor, B. Rodmacq, C. Ducruet, C. Portemont, I. L. Prejbeanu, and B. Dieny, IEEE Trans. Magn. **46**, 1412 (2010).
[18]H. X. Yang, M. Chshiev, B. Dieny, J. H. Lee, A. Manchon, and K. H. Shin, Phys. Rev. B **84**, 054401 (2011).
[19]T. Liu, J. W. Cai, and L. Sun, AIP Advances **2**, 032151 (2012).